CrystEngComm

Accepted Manuscript

ROYAL SOCIETY OF CHEMISTRY

www.rsc.org/crystengcomm

Cite this: DOI: 10.1039/c0xx00000x

www.rsc.org/xxxxxx

ARTICLE TYPE

NaV_2O_5 crystals of right-angle-shaped nanostructure assembly

Tie-Zhen Ren,*[a] Zhanbing He,*[b] Hongjie Fan,[a] Huanrong Li,[a] and Zhong-Yong Yuan*[c]

Received (in XXX, XXX) Xth XXXXXXXXX 20XX, Accepted Xth XXXXXXXXX 20XX
DOI: 10.1039/b000000x

L-shaped NaV_2O_5 crystals with two straight arms were controllably synthesized in a hydrothermal system with the assistance of 1,3,5-benzentricarboxylate acid (H_3BTC). The arms were assembled by nanowires grown along *b*-direction. By means of transmission electron microscopy, the (310) twin boundary was found to connect the nearly perpendicular arms to form the *L*-shaped structure. Meanwhile the *L*-shaped crystallites, as the basic unit, can be further self-assembled into ⊣ and ┼ shapes.

Introduction

Understanding the mechanisms of growth and crystallization at nanoscale to further explore fundamental properties and potential applications of functional nanomaterials have always been the research focus of nanotechnology and material science. From the structure to properties, the suitable morphology may give impressive influence on the property of the inorganic crystals.[1-5] Pursuing the special application, solid materials have been synthesized in many structures, ranging from conventional metal colloids [6] to modern near-monodispersed nanoclusters,[7,8] shape-controlled nanocrystals,[9] nanowires/belts/rods,[5,10,11] sheets,[12] tubes,[13,14] hierarchical dendrites[15,16] and nanoporous architectures.[17] Among all these different morphologies, the controlled growth of anisotropic inorganic nanomaterials has attracted particular interest due to their outstanding and stable electric, optical and photovoltaic properties. Some unusual structures were observed, even infrequent in nature. For instance, porous hematite (α-Fe_2O_3) with branched nanostructures such as V and Y shapes have been prepared through dehydration of goethite (α-FeOOH) precursor.[18] However, their low quantity production can not be expected for further application. SnO_2 and GaSe zigzag belts/wires could be obtained only under high temperature and Ar gas protection,[19] or through the special vapor-liquid-solid (VLS) growth process,[20] which restrict their commercial production and practical application.

NaV_2O_5 is of great interest due to its spin-Peierls behavior and unique optical and magnetic properties.[21,22] The analogue compound $Na_xV_2O_5$ represents as well the ladder structure and its optical properties can be adjusted by the loading of Na ions, which corresponds to the variable valence of V ions.[23,24] The vanadium atoms in NaV_2O_5 are characterized by a two-leg ladder that is consisted of two -V–O2–V– chains along the b-axis.[25,26] The common nanobelt-shape and needle-like particles have been prepared in several techniques, such as solid-state reaction[27] and hydrothermal methods.[28] It was reported that the presence of F^- was critical for the formation of NaV_2O_5 needles along the <0 1 0> axis.[28] In this paper, we present a systematic investigation of the formation of *L*-shaped NaV_2O_5 crystals by a facile hydrothermal synthesis route. A special twinning structure with ~90° arrangement of assembled nanowires, which has scarcely been reported in inorganic crystalline materials, was observed. It is found that the 1,3,5-benzentricarboxylate acid (H_3BTC) in a range of alkali solution favours the formation of *L*-shaped structure.

Experimental

Synthesis

In a typical synthesis of *L*-shaped NaV_2O_5 crystals, 2 mmol of H_3BTC was mixed with 3.5 ml of NaOH solution (2 M) in 20 ml of water and 5 ml of ethanol under stirring at room temperature for 30 min, followed by the addition of 4 mmol of NH_4VO_3 to get yellow gel (pH = 7.5 – 7.7). After further stirring for 40 min, the mixture was transferred into a Teflon-lined autoclave, and heated at 180 °C for 3 – 90 days. The products were collected, washed with water and dried.

Characterization

X-ray diffraction (XRD) patterns were recorded on a Rigaku D/max-2500 diffractometer with Cu-K_α radiation, operated at 40 kV and 100 mA. Scanning electron microscopy (SEM) was taken on a Shimadzu SS-550 microscope at 15 kV. Transmission electron microscopy (TEM) was carried out on a Jeol JEM 2010 microscope, working at 200 kV. A trace amount of sample was dispersed in ethanol solution by sonication for 10 min, and then deposited on a carbon-coated copper grid, which was used as a TEM specimen.

Thermogravimetry (TG) and differential scanning calorimetry (DSC) were performed using a TA SDT Q600 instrument at a heating rate of 5°/min using α-Al_2O_3 as the reference. The chemical compositions of Na and V were analyzed by inductively coupled plasma (ICP) emission spectroscopy on a Thermo Jarrell-Ash ICP-9000 (N+M) spectrometer.

Results and discussion

The *L*-shaped NaV_2O_5 crystals were synthesized in a

hydrothermal system with NH_4VO_3/H_3BTC molar ratio of 2 : 1 and pH of 7.5 – 7.7 at 180 °C. By ICP mass spectrometry analysis, the weight percentage of Na and V is 9.8% and 43.9%, respectively, suggesting the molecule formula of $Na_xV_2O_5$ (x = 0.9893). Fig. 1a shows a typical SEM image of the synthesized $Na_xV_2O_5$ crystallites. Each particle is *L*-shaped, having two orthogonal arms with the length of around 500 μm. The energy-dispersive X-ray spectroscopy (EDS) (Fig. S1, ESI†) indicates V, Na and O elements. The XRD pattern (Fig. 1b) is indexed well as an orthorhombic NaV_2O_5 (PDF# 70-0870, space group: $P2_1mn$, a = 1.132 nm, b = 0.360 nm, c = 0.480 nm). The strong and sharp diffraction peaks suggest the high crystallization of the material. The enlarged images in Fig. 1c and d show that the arms of the *L*-shape are composed of substructures, which could be further confirmed as aligned nanowires *infra*. The two arms are jointed in one end with a representation of a dark line (as indicated by green arrows in Figs. 1d-f) to form an *L*-shape. Take a closer inspection from the enlarged connected area in Fig. 1e, it is found small *U*-typed blocks located in each arm and grew along two vertical directions, e.g. where in the red dash lines in Figs. 1e and f. The *U*-typed block is formed due to the two ends of one short arm of the *L*-shaped substructure are both connected by another arm, as schematically illustration in the red dash area in Fig. 1f. In other words, the *L*-typed substructure can be further assembled into a *U*-typed structure.

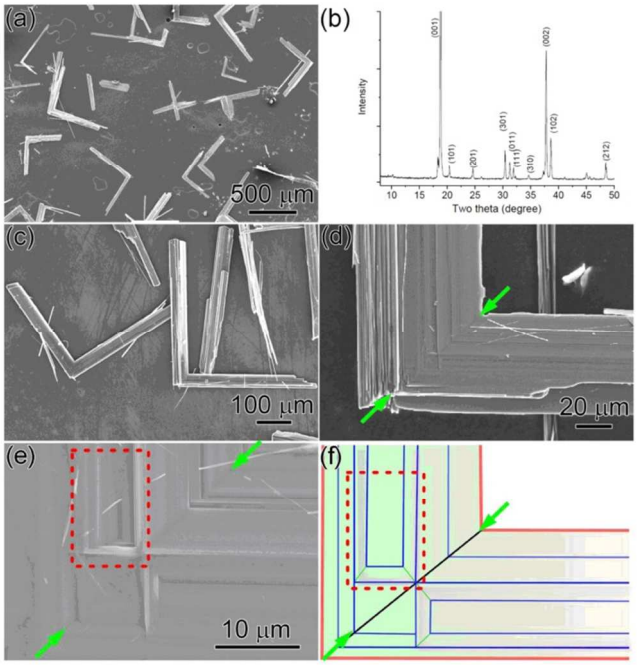

Fig. 1. (a), (c), (d) SEM images of *L*-shaped crystals at different magnifications. The arms are straight and have the same diameter for each crystalline. (b) Powder XRD pattern of *L*-shaped crystals. (e) High-magnification SEM image of the crystal in (d) to show the details of the connected area of two arms. (f) A schematic of the connected area of two arms in (d). A dark line, as highlighted by green arrows, is found to connect the nearly perpendicular arms of the *L*-shaped crystals.

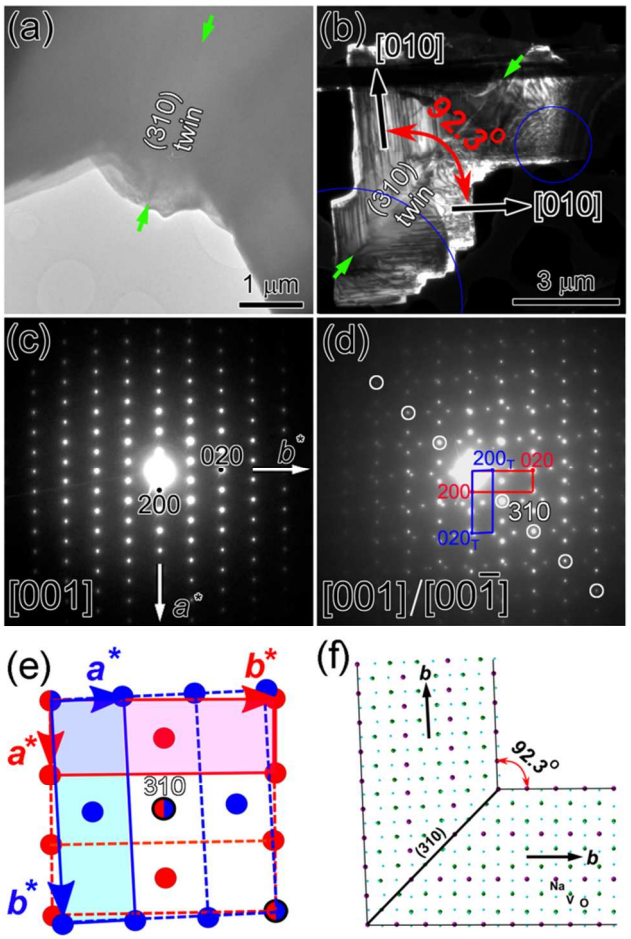

Fig. 2. (a) Bright-field TEM image of the connected area of one L-typed crystallite. The dark line connecting two arms is (310) twin boundary. (b) Dark-field TEM image of one thin sample from the connected area of one *L*-typed crystalline. The nanowire-like contrast is shown in two portions beside the (310) twin boundary. (c) [001] EDP from one portion in (b) showing its characteristic of one single crystal. (d) [001] EDP from two portions in (b) showing a rotation twin. (e) An enlarged schematic of (d) to clearly show the relationship of two sets of EDPs. (f) A structural model of the *L*-typed NaV_2O_5. The angle of b direction of two arms is good in agreement with the experimental result in (b), (d) and (e).

In order to elucidate the reason of the *L*-shaped connection, TEM was performed. Fig. 2 is a low magnification TEM image of the connected area of one *L*-shaped NaV_2O_5 crystallite. The ~90° connection of the two parts separated by a dark line (as indicated by two green arrows) is corresponding to the connected area in the SEM images in Fig. 1. Selected-area electron diffraction pattern (EDP) indicates the growth direction of each arms is along b direction and the dark line is corresponding to a (310) twin boundary (Fig. S2, ESI†), suggesting that the arms of *L*-shaped NaV_2O_5 crystallites are connected through one (310) twin boundary. In order to reveal more about the connected area by TEM, a thinner area consisting of the twin boundary is selected (Fig. 2b). Both the nanowire-like substructure and (310) twin boundary are clearly seen in the dark-field image in Fig. 2b. The orientation of the nanowire-like substructure at both parts beside the twin boundary is determined as [010] by EDPs (Fig. 2c), but rotated by 92.3°. Fig. 2d is the EDP containing twin boundary. It has two sets of EDPs (as highlighted by red and blue

rectangular respectively) with ± *n* (310) diffraction spots, where *n* is integer shared by both, e.g. those in the white circles. A schematic in Fig. 2e shows details of the relationship of two sets of EDPs in Fig. 2d. The shared (310) diffraction spot implies a (310) twin boundary. The deviation of 2.3° of the blue *a** from the red *b** suggests the angle of the *b* axis of two parts beside the twin boundary is 92.3°, being in good agreement with that of the nanowire-like substructure in Fig. 2b. Based on the TEM analysis, a structural model of the (310) twin boundary is shown in Fig. 2f. The growth direction of each arm is along *b*, and the angle between them is 92.3° when the (310) twin boundary is resulted, consistent well with the experimental results.

Under some conditions such as compress stresses, ultrasonic, the arms of *L*-shaped crystallites could be dispersed into a bunch of nanowires (Figs. 3a and b), revealing the assembly of nanowires into the arms. Fig. 3c is a TEM image of one bunch of nanowires from one arm. The nanowires are assembled, but with the same b growth direction. Fig. 3d shows the dispersed nanowires when the samples were treated by ultrasonic in alcohol. The growth direction of the nanowires is determined as [010] again from EDPs. The [010] growth direction is also directly confirmed from [001] high resolution transmission electron microscope (HRTEM) image in Fig. 3e.

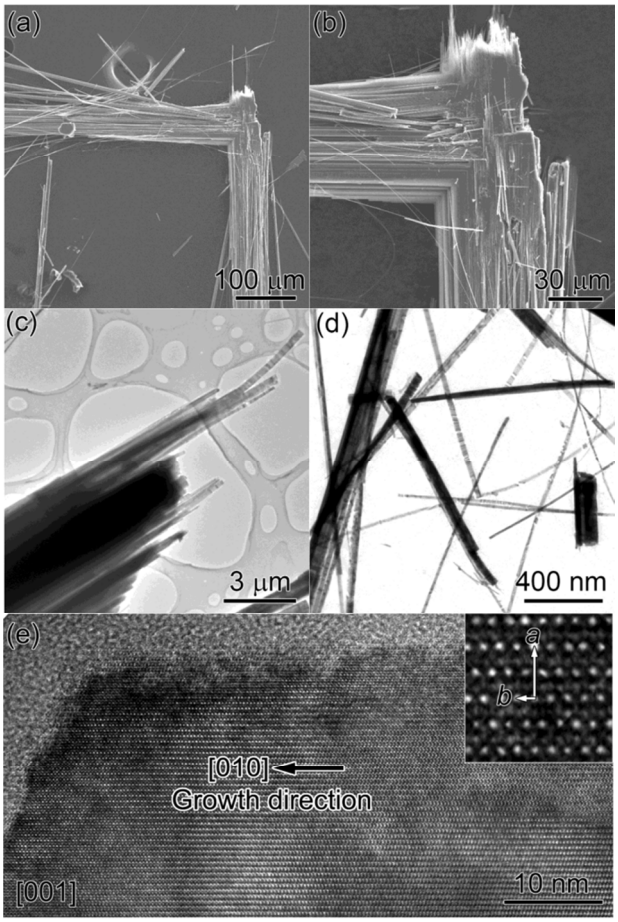

Fig. 3. (a) and (b) SEM image of one L-shaped crystalline with arms showing a bunch of nanowires; (c), (d) TEM images showing nanowires from the arms; (e) The [001] HREM image of one nanowire, one enlarged image with indicated *a* and *b* is inserted.

The growth of nanorods has been reported during the hydrothermal treatment in a normal case,[29,30] but the well-packed nanowires to form a ~90° twin crystal have not been observed yet in the soft chemical environment.[31,32] Moreover, as the derivation of *L*-shaped crystals, the ⊣ and ⊥ types can also be obtained with the increase of hydrothermal time (Fig. 4). Such more complex structures are the results of the further packing of the basic L-shaped structure, as illustrated in Fig. 5. The *U*-typed blocks in the red dash area in Figs. 1e and f are also the result of the further packing of the basic *L*-shaped structure.

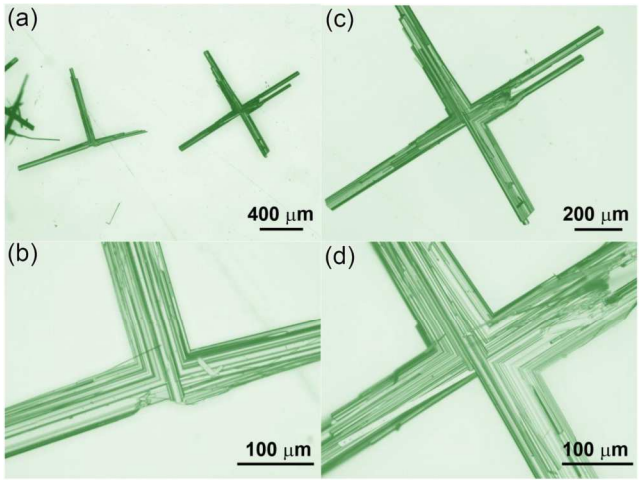

Fig. 4. Optical images of⊣ -shape and ⊥-shape particles derived from *L*-shape particles.

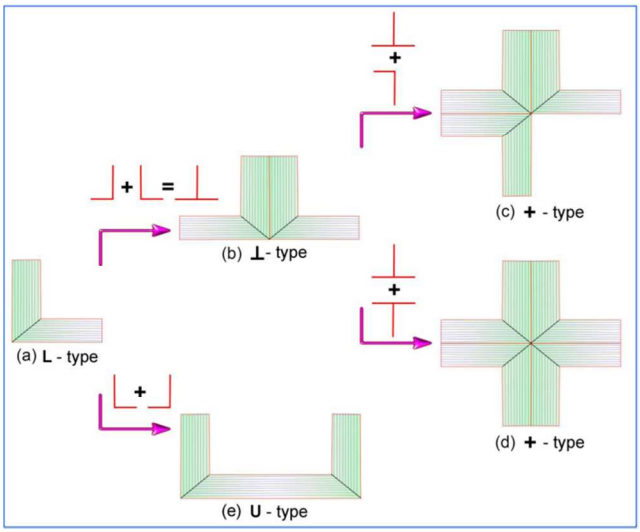

Fig. 5. The scheme of the packing mode from L-shape to ⊣ -shape and ⊥- shape, etc.

For optimizing the growing conditions of the *L*-shaped crystals, a series of parallel experiments were carried out, as summarized in Table S1 (ESI†). It is found that the organic molecule affects the morphology of NaV_2O_5. No compound can be produced in the absence of the organic molecules. Some congeneric organics, such as phthalic acid and terephthalic acid, can not give a useful contribution on the formation of *L*-shape NaV_2O_5 crystals, though a small quantity of *L*-shape crystals with low quality were observed when pyromellitic acid was used in the synthesis (Fig. S4, ESI†). In contrast, trimesic acid in the pH range of 7-9 could be effective for the production of *L*-shaped

crystals and the rod- and needle- shaped crystals were easy to be prepared at pH lower than 5 or higher than 11. Moreover, the optimized hydrothermal temperature is in the range of 160-190 °C. Lower or higher temperature can only produce either gel or bulk samples. Meanwhile, the optimized molar ratio of NH_4VO_3 and TMB is 1 - 2. The higher or lower molar ratio just resulted in the formation of the plate shape product or mixtures (Fig. S5, ESI†). Especially, the *L*-shaped crystals were observed with the size of 50 μm by hydrothermal treatment of three days (Fig. S6, ESI†), which enlarged into 500 μm after three months.

The crystal structure of NaV_2O_5 consists of double chains of edge-sharing distorted tetragonal VO_5 pyramids running along the orthorhombic *b* axis, which are linked together via common corners of the pyramids to form sheets and fit space group $P2_1mn$. The layers of edge/corner-sharing tetragonal VO_5 pyramids connected in the *a* - *b* plane are stacked along the *c*-axis of the structure, while the Na^+ ions are situated between these layers. The twist boundary and dislocations may introduce distortion in the layers of VO_5 pyramids along [001] direction.[33] V_2O_5 in the structure of NaV_2O_5 forms pyramids, with V inside the pyramid and O sites on the four corners of the basal plane and at the apex. The Na atom donates one extra electron to the structure that is shared between the two V atoms, partially filling a band derived from V *dxy* orbitals.[26] The alternating chains of nonmagnetic V^{5+} ions and magnetic V^{4+} ones ($3d^1$, s=1/2) results formally in a random distribution of V^{4+} and V^{5+} ions, or in a localization of electrons on V-O-V molecular orbital on the rungs of the ladders running along the *b*-axis, which leads to the formation of *L*-shape crystal at (310) plane under the effect of aromatic acid at the specific pH condition (Fig. S7, ESI†). It is thus proposed that the nanorods grow up with the ladder structures, and the self-assemble procedure between the nanorods and the arrangement of those nanorods by turning 90° undertakes simultaneously in this system.

Conclusions

The *L*-shaped NaV_2O_5 crystals were synthesized on a large scale via a facile hydrothermal treatment technique. The ladder structure is the self-driven force to form the twinning structure with 92.3º at lap joint under the assistance of the trimesic acid. The organic species H_3BTC and a suitable pH condition are crucial in producing the *L*-shaped crystals. The crystal size can be adjusted by the hydrothermal reaction time. The observed special twin angle in the crystals rests with both the reaction condition and the ladder structure of NaV_2O_5. The further packing of the *L*-shaped particles into the ⊣ and ┼ types can be obtained. This unusual phenomenon may inspire the fabrication of the materials with the special morphologies for practical applications.

Acknowledgements

This work was supported by the NSFC (21076056), the Program for Innovative Research Team in University (IRT1059), the 111 project (B12015), and the Fundamental Research Funds for the Central Universities (06111022). The authors also thank Dr. Shuying Piao in Bruker for the help of electron microscopy.

Notes and references

[a] *School of Chemical Engineering and Technology, Hebei University of Technology, Tianjin 300130, China. E-mail: rtz@hebut.edu.cn*
[b] *State Key Laboratory for Advanced Metals and Materials, University of Science and Technology Beijing, Beijing 100083, China. E-mail: hezhanbing@ustb.edu.cn*
[c] *Key Laboratory of Advanced Energy Materials Chemistry (Ministry of Education),Collaborative Innovation Center of Chemical Science and Engineering (Tianjin), College of Chemistry, Nankai University, Tianjin 300071, China. E-mail: zyyuan@nankai.edu.cn*

† Electronic Supplementary Information (ESI) available: Experimental details and the resultant morphology, formation mechanism. See DOI: 10.1039/b000000x/

1 X. Peng, L. Manna, W. Yang, J. Wickham, E. Scher, A. Kadavanich, A. P. Alivisatos, *Nature* 2000, **404**, 59.
2 G. H. Du, F. Xu, Z. Y. Yuan, G. van Tendeloo, *Appl. Phys. Lett.* 2006, **88**, 243101.
3 A. P. Alivisatos, *Science* 1996, **271**, 933.
4 D. H. Zhang, Q. P. Wang, Z. Y. Xue, *Appl. Surf. Sci.* 2003, **207**, 20.
5 N. A. Melosh, A. Boukai, F. Diana, B. Gerardot, A. Badolato, P. M. Petroff, J. R. Heath, *Science* 2003, **300**, 112.
6 G. Schön, U. Simon, *Colloid Polym. Sci.* 1995, **273**, 202.
7 A. Roucoux, J. Schulz, H. Patin, *Chem. Rev.* 2002, **102**, 3757.
8 H. Yu, P. C. Gibbons, K. F. Kelton, W. E. Buhro, *J. Am. Chem. Soc.* 2001, **123**, 9198.
9 T. S. Ahmadi, Z. L. Wang, T. C. Green, A. Henglein, M. A. El-Sayed, *Science* 1996, **272**, 1924.
10 N. R. Jana, L. Gearheart, C. J. Murphy, *Adv. Mater.* 2001, **13**, 1389.
11 Y.-J. Han, J. M. Kim, G. D. Stucky, *Chem. Mater.* 2000, **12**, 2068.
12 M. Shirai, K. Igeta, M. Arai, *Chem. Commun.* 2000, 623.
13 M. Prato, *Nature* 2010, **465**, 172.
14 Z. Ren, G. Xu, Y. Liu, X. Wei, Y. Zhu, X. Zhang, G. Lv, Y. Wang, Y. Zeng, P. Du, W. Weng, G. Shen, J. Z. Jiang, G. Han, *J. Am. Chem. Soc.* 2010, **132**, 5572.
15 D. Kuang, A. Xu, Y. Fang, H. Liu, C. Frommen, D. Fenske, *Adv. Mater.* 2003, **15**, 1747.
16 W. Qingqing, X. Gang, H. Gaorong, *Crystal Growth Design* 2006, **6**, 1776.
17 X. Wei, G. Xu, Z. Ren, C. Xu, W. Weng, G. Shen, G. Han, *J. Am. Ceram. Soc.* 2010, **93**, 1297.
18 H. Yang, X. Mao, Y. Guo, D. Wang, G. Ge, R. Yang, X. Qiu, Y. Yang, C. Wang, Y. Wang, G. Liu, *CrystEngComm* 2010, **12**, 1842.
19 L. Li, K. Yu, J. Wu, Y. Wang, Z. Zhu, *Cryst. Res. Technol.* 2010, **45**, 539.
20 H. Peng, S. Meister, C. K. Chan, X. F. Zhang, Y. Cui, *Nano Lett.* 2007, **7**, 199.
21 A. Meetsma, J. L. De Boer, A. Damascelli, J. Jegoudez, A. Revcolevschi, T. Palstra, *Acta Crystallogr., Sect. C: Cryst. Struct. Commun.* 1998, **54**, 1558.
22 X. Ming, H.-G. Fan, Z.-F. Huang, F. Hu, C.-Z. Wang, G. Chen, *J. Phys.: Cond. Matter* 2008, **20**, 155203.
23 M. Onoda, Y. Mizuguchi, *J. Phys.: Cond. Matter* 2008, **20**, 445207.
24 R. P. Ozerov, V. A. Streltsov, A. N. Sobolev, B. N. Figgis, V. L. Volkov, *Acta Crystallogr., Sect. B: Struct. Sci.* 2001, **57**, 244.
25 K. Ohwada, Y. Fujii, J. Muraoka, H. Nakao, Y. Murakami, Y. Noda, H. Ohsumi, N. Ikeda, T. Shobu, M. Isobe, Y. Ueda, *Phys. Rev. B* 2007, **76**, 094113.
26 J. Spitaler, E. Y. Sherman, C. Ambrosch-Draxl, *Phys. Rev. B* 2007, **75**, 014302.
27 I. Loa, A. Grzechnik, U. Schwarz, K. Syassen, M. Hanfland, R. K. Kremer, *J. Alloys Compounds* 2001, **317–318**, 103.
28 F. Hu, X. Ming, G. Chen, C. Wang, A. Li, J. Li, Y. Wei, *J. Alloys Compounds* 2009, **479**, 888.
29 G. Du, Q. Chen, R. Che, Z. Yuan, L.-M. Peng, *Appl. Phys. Lett.* 2001, **79**, 3702.
30 S. A. Corr, M. Grossman, Y. Shi, K. R. Heier, G. D. Stucky, R. Seshadri, *J. Mater. Chem.* 2009, **19**, 4362.
31 C. Cayron, M. D. Hertog, L. Latu-Romain, C. Mouchet, C. Secouard, J.-L. Rouviere, E. Rouviere, J.-P. Simonato, *J. Appl. Crystallogr.* 2009, **42**, 242.
32 M. S. Whittingham, *Curr. Opin. Solid State Mater. Sci.* 1996, **1**, 227.
33 Y. G. Wang, H. Y. Wu, V. P. Dravid, *J. Mater. Sci.* 2005, **40**, 1725.

Graphic abstract

L-shaped NaV_2O_5 crystals with two straight arms of nanowire assembly were controllably synthesized, and the (310) twin boundary was found to connect the nearly perpendicular arms to form the *L*-shaped structure.